Cure Modeling and Monitoring of Epoxy/Amine Resin Systems. II. Network Formation and Chemoviscosity Modeling

PANAGIOTIS I. KARKANAS, IVANA K. PARTRIDGE

Advanced Materials Department, School of Industrial and Manufacturing Science, Cranfield University, Bedford, MK43 0AL, United Kingdom

Received 12 March 1999; accepted 19 September 1999

ABSTRACT: The glass transition temperature (T_g) advancement and the chemoviscosity development under isothermal conditions have been investigated for four epoxy/amine systems, including commercial RTM6 and F934 resins. Differential scanning calorimetry (DSC) was the thermoanalytical technique used to determine the T_g advancement and rheometry the technique for the determination of the chemoviscosity profiles of these resin systems. The complex cure kinetics were correlated to the T_g advancement via an one-to-one relationship using Di Benedetto's formula. It was revealed that the three-dimensional network formation follows a single activated mechanism independent of whether the cure kinetics follow a single or several activation mechanisms. The viscosity profiles showed the typical characteristics of epoxy/amine cure. A modified version of the Williams-Landel-Ferry equation (WLF) was adequate to model the viscosity profiles of all the resin systems, in the temperature range 130 to 170°C, with a very good degree of accuracy. The parameters of the WLF equation were found to vary in a systematic manner with cure temperature. Further correlation between T_g and viscosity showed that gelation, defined as the point where viscosity reaches 10^4 Pas, occurs at a unique T_g value for each resin system, which is independent of the cure conditions. © 2000 John Wiley & Sons, Inc. J Appl Polym Sci 77: 2178–2188, 2000

Key words: epoxy/amine resin systems; network formation; chemoviscosity modeling

INTRODUCTION

Network Formation

The major physical transformations that occur during thermoset cure, gelation and vitrification, are important parameters in the processing of the corresponding fiber reinforced composites. Whether or not a particular thermoset resin system is suitable for a given fiber-reinforced composite processing technique depends critically on its viscosity evolution during the processing cycle. For autoclave fabrication of composite parts, knowledge of the viscosity profile gives guidance on when the pressure should be applied during the cure cycle (prior to gelation), to achieve part consolidation without excessive resin flow. For resin transfer molding (RTM), the viscosity of the resin at the early stages of the cure is an additional concern. The requirements for successful mold filling are low resin viscosity for satisfactory impregnation of the preform and long pot life. Therefore, knowledge of the evolution of rheological properties of curing thermosets is essential for their success-

Correspondence to: I. K. Partridge.

Contract grant sponsor: DTI/EPSRC Structural Composites LINK Program; contract grant number: GR/J96222.

Journal of Applied Polymer Science, Vol. 77, 2178–2188 (2000)

ful application. Determination of the end of the cure is also a key issue in the composite industry. Vitrification times indicate the completion of the cure at the cure cycle of interest.

An epoxy–amine system, which is a polyfunctional system, produces infinite networks during the cure reaction. At the initial stages of the cure a number of high molecular weight particles are formed, which are dispersed in a low molecular weight phase that constitutes the continuous phase. The number and molecular weights of these particles increase as the cure reaction proceeds, and crosslinking becomes operative. The point where the growth and branching of polymer chains, caused by intramolecular reactions, causes a phase transition from the liquid state to the rubbery state is called "gelation." This transformation is a critical point in resin cure. It occurs at a specific point of chemical conversion, and depends on the curing system itself and the environment in which the reaction takes place.[1]

Many other changes in the physical state of the epoxy–amine system take place during the cure reaction as a consequence of the changes in the free volume and in the glass transition temperature of the reactive system. During cure to full conversion at isothermal conditions, the glass transition temperature (T_g) increases from the value representative of the uncured monomer mixture (T_{g0}) to the fully cured value ($T_{g\infty}$). Molecular gelation is a transition that occurs at an intermediate T_g value between T_{g0} and $T_{g\infty}$, that of ${}_{\text{gel}}T_g$. When the isothermal cure temperature, T_c, is much lower than the $T_{g\infty}$, the reaction generally becomes diffusion controlled as T_g increases through T_c and a limiting value of T_g is obtained. This gradual cessation of the reaction marks the transition from the rubbery to the glassy state of the curing material. The resin eventually solidifies, and no further reaction will take place unless it is triggered by a further increase in the curing temperature. This transition, which will occur when T_g reaches T_c, is defined as "vitrification," and be considered as the identification of the end of the cure. Graphical representation of the above phenomena on the well-known Time–Temperature–Transformation (TTT) diagram, which was first adopted for the epoxy resin cure by Gillham,[2] provides an intellectual framework for the understanding of the curing process and the optimization of the processing and the final material properties.

The most comprehensive expression that correlates segmental mobility and chemical conversion with T_g, is the expression derived by Adabbo and Williams[3] using Di Benedetto's equation,[4] and has the form of:

$$\frac{T_g - T_{g0}}{T_{g0}} = \frac{\left(\frac{E_x}{E_m} - \frac{F_x}{F_m}\right) \cdot X_g}{1 - \left(1 - \frac{F_x}{F_m}\right) \cdot X_g} \quad (1)$$

where E_x and E_m are the lattice energies for crosslinked and uncrosslinked polymer respectively, F_x and F_m are the corresponding segmental mobilities, and X_g is the extent of conversion at T_g.

Chemoviscosity Modeling

For a thermoplastic material, the viscoelastic properties are fully determined by shear rate, processing temperatures, and the flow geometry. For a thermosetting resin the rheology is influenced by additional factors: the reaction kinetics of the resin system and the elapsed cure time. The effects of temperature and time on chemoviscosity can be described in terms of the extent of cure (α) by knowing the kinetics of the cure, $\alpha(T, t)$.

Much work has been done to determine the appropriate mathematical models that best describe the viscosity advancement of epoxy resins during cure. They range from empirical models,[5,6] probability based models,[7,8] gelation models,[9,10] to models based on free volume analysis.[11]

The most commonly used empirical model has the form:[5]

Isothermal conditions: $\ell n\,\eta(t)$

$$= \ell n\,\eta_\infty + \frac{\Delta E_\eta}{RT} + t k_\infty \exp\left(\frac{\Delta E_k}{RT}\right)$$

Nonisothermal conditions: $\ell \mathrm{n}\eta(\mathrm{t})$

$$= \ell n\,\eta_\infty + \frac{\Delta E_\eta}{RT} + \int_0^t k_\infty \exp\left(\frac{\Delta E_k}{RT}\right) dt \quad (2)$$

where: $\eta(t)$ the viscosity as a function of time at temperature T, η_∞ is the projected viscosity of the fully cured resin, ΔE_η is the Arrhenius activation energy for viscosity, R is the Universal gas constant, T is the absolute temperature, t is the cure time, k_∞ is the kinetic analog of η_∞, and ΔE_k is the kinetic analog of ΔE_η.

A more comprehensive expression, incorporating probabilistic considerations of the macromolecular network formed during the cure, is:[8]

$$\ell n\,\eta = \ln A + \frac{D}{RT} + \left(S + \frac{C}{RT}\right)\ell n\,\frac{\overline{MW}}{MW_0} \quad (3)$$

where A, D, S, and C are fitting parameters and $\overline{MW}$, MW_0 are the weight average molecular weight and the molecular weight at zero conversion, respectively.

Expressions that use information such as the degree of cure at the gel point, α_{gel}, have also been used for viscosity modeling. A suitable example is the one derived by Castro and Macosko:[9]

$$\eta = \eta_0\left(\frac{\alpha_{gel}}{\alpha_{gel} - \alpha}\right)^{A+B\alpha} \quad (4)$$

In this expression, η_0 is the initial viscosity at temperature T, prior to the start of the cure, and A and B are fitting parameters.

Another expression that has been used extensively in viscosity modeling is the Williams-Landel-Ferry equation (WLF), which has the well-known form:[12]

$$\ell n\,\frac{\eta(T)}{\eta(T_s)} = -\frac{C_1(T - T_s)}{C_2 + T - T_s} \quad (5)$$

where $\eta(T)$ and $\eta(T_s)$ are the viscosities at temperatures T and T_s, respectively, and C_1, C_2 are constants independent of temperature.

The special characteristics of thermoset cure, such as the increase of the glass transition temperature due to network formation, have been incorporated into the WLF equation resulting in a variety of expressions similar to the original one, such as the one used by Mijovic and Lee:[13]

$$\ell n\,\frac{\eta}{\eta_g} = -\frac{C_1(T)[T - T_g(T, t)]}{C_2(T) + T - T_g(T, t)} \quad (6)$$

Halley and Mackay,[14] in their extensive overview of the chemorheology of thermosets, have summarized the rheological models applied to thermoset cure along with the models for shear rate and filler effects, which range from simple power law models to more complicated models incorporating WLF terms.

EXPERIMENTAL

Materials

Four different epoxy-based resin systems were used in this study. Two of them were commercially available epoxy/amine systems, whereas the other two were specially prepared experimental systems based on one epoxy resin and two amine hardeners.

The two commercial resins used were RTM6, used for RTM applications and F934, a chemical matrix resin for carbon fibre prepregs. The other two resin systems, RMO and RMO2, were especially prepared in the laboratory, as mixtures of a tetrafunctional epoxy resin (MY721 supplied by Hexcel Composites UK) and different proportions of two amine hardeners (M-MIPA and M-DEA, supplied by LONZA Ltd.). Further details of the materials and the formulations used are given elsewhere.[15]

Methods

For the determination of the cure kinetics and the T_g, the resins were cured isothermally at various temperatures in the range between 130 to 170°C. Calculation of the reaction kinetics were made from both direct isothermal DSC experiments and measurements of residual heats of reaction of partially cured samples. The complete experimental setup and the method for determining the cure kinetics under isothermal conditions are given elsewhere.[15]

Estimations of the T_g of the partially or fully cured resins were made from the results of the residual heat of reaction experiments. The glass transition temperature was determined as the midpoint of the endothermic shifts observed during the rescans of the partially cured resin. At the later stages of the cure, when the resin has reached vitrification, the residual reaction exotherm starts in the immediate vicinity of the T_g region. This made the determination of the glass transition and subsequently of the residual heat of reaction difficult. Because of the above difficulty, the T_g results will be presented in the following sections as approximate values of the actual T_g values.

The viscosity of all the resin systems was measured during the course of cure using a Bohlin Instruments CVO-10 rheometer. The measuring geometry used was a 40 mm parallel plate system with the bottom plate fixed and the top plate

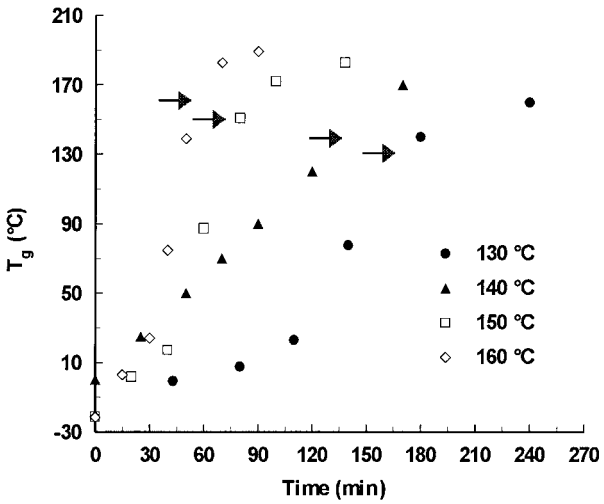

Figure 1 Glass transition temperature profile of RMO2 resin at different cure temperatures.

oscillating at a fixed frequency. The measurements were made by controlling the applied stress so that the corresponding strain never exceeded predetermined limits. Prior to each experiment, frequency and stress sweeps were made to determine the appropriate frequency and stress ranges within which the curing resin behaved as a linearly viscoelastic material.

All experiments were conducted under isothermal conditions at temperatures of 130, 140, 150, and 160°C. After preheating the plates to the experimental temperature, the resin was placed on the bottom plate and the upper plate was lowered down until a fixed gap of 0.5 mm between the plates had been reached. After allowing 2–3 min for temperature equilibrium to establish, the measurement was started, collecting the viscosity response at fixed time intervals. When the measured viscosity had exceeded the value of 20 kPas, the measurement was stopped and the data were stored for subsequent analysis.

Control of the temperature was made by an electrical heater with two individual heating elements, one for each plate. To prevent any heat losses, a specially designed insulating system was used, enclosing the measuring unit. Because the measuring parallel plates would be firmly bonded and irrecoverable at the end of the experiments, disposable plates were used. These plates can withstand high temperatures and after each experiment the cured resin was burned off at 500°C to recover the plates.

RESULTS AND DISCUSSION

T_g Advancement

Typical profiles of the T_g advancement at different cure temperatures for the RMO2 resin system are shown in Figure 1 as plots of T_g against cure time. The arrows indicate the vitrification points at each cure temperature, as these are defined by $T_g = T_c$. As can be seen in these figures, the final T_g is different at each cure temperature. This is the result of the diffusion control of reaction kinetics, which becomes significant after the vitrification point has been reached. The reaction is hindered because of structural limitations, which become more pronounced at low cure temperatures, where the energy supplied to the curing system is lower. The shape of the plots follows a similar trend with the conversion profiles (see Fig. 2), indicating the high correlation between these two properties. Any changes in the cure advancement have a direct impact on the T_g of the resin. An observation that was made during the evaluation of the T_g and the conversion at the later stages of the cure was the relative accuracy of the measurements. The endothermic shift at the T_g region is easily determined by DSC, whereas the residual heat of reaction is not. This makes the determination of the T_g more accurate than the calculation of the conversion at these stages of the cure.

The interrelation between T_g and cure advancement can be seen in Figure 3, where the cure advancement has been plotted against the

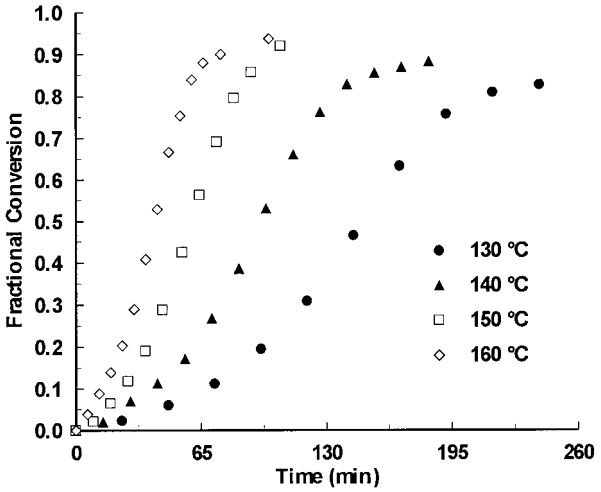

Figure 2 Fractional conversion vs. cure time of RMO2 resin under isothermal cure at different temperatures (from ref. 15).

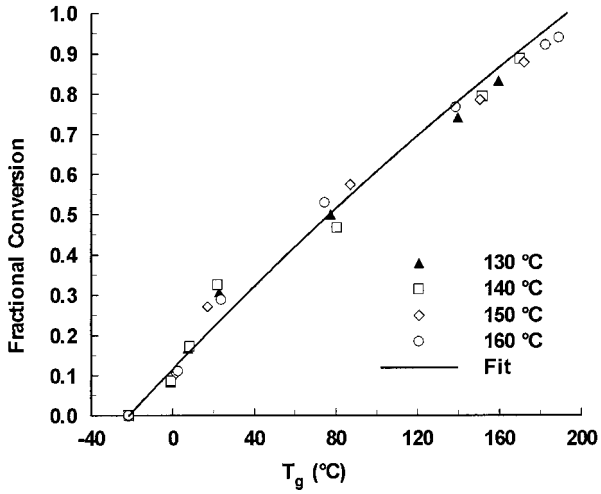

Figure 3 Plots of fractional conversion vs. T_g for the cure of RMO2 resin. The fit was produced by eq. (7).

glass transition temperature for the RMO2 resin system. The one-to-one relationship is evidenced by the formation of master curve. For all the resin systems, there exists a unique master curve, independent of the cure temperature, that is followed throughout the cure. The significant scatter in the data at the later stages of the cure is attributed to the lower sensitivity of the DSC in measuring the level of conversion compared to that of the T_g measurement.

The relationship between T_g and conversion given by eq. (1) can be expressed as:

$$T_g = T_{g0} + \frac{(T_{g\infty} - T_{g0})\lambda\alpha}{1 - (1 - \lambda)\alpha} \quad \text{where} \quad \lambda = \frac{F_x}{F_m} \tag{7}$$

by using:

$$\frac{E_x/E_m}{F_x/F_m} = \frac{T_{g\infty}}{T_{g0}} \tag{8}$$

eq. (7) can be used to model the T_g-conversion relationship by treating λ as an adjustable parameter. The resulting values of λ from the application of this expression to the experimental data are given in Table I for all the resin systems investigated. The corresponding fitting results for the RMO2 resin only are shown in Figure 3.

If the curing reaction is chemically controlled, that is if there are no contributions from diffusion control, then the reaction rate can be expressed as:

$$\frac{d\alpha}{dt} = k(T) \cdot f(\alpha) \tag{9}$$

where $k(T)$ is the reaction rate constant, which is a function of temperature and $f(\alpha)$ is some function of conversion. Integration of the above expression at constant temperature and taking the natural logarithm will give:

$$\ell n\left(\int_0^\alpha \frac{d\alpha}{f(\alpha)}\right) = \ell nk(T) + \ell nt \tag{10}$$

The left-hand side of this expression is a function only of conversion, or if we consider the one-to-one relationship between conversion and T_g, a function only of T_g. Thus:

$$F(T_g) = \ell nk(T) + \ell nt \tag{11}$$

Because the function F depends only on T_g, for the cure at two different temperatures, T_1 and T_2, it follows that:

$$\begin{aligned} F(T_g) &= \ell nk(T_1) + \ell nt_1 \\ &= \ell nk(T_2) + \ell nt_2 \Rightarrow \ell nA - \frac{E}{R}\frac{1}{T_1} + \ell nt_1 \\ &= \ell nA - \frac{E}{R}\frac{1}{T_2} + \ell nt_2 \Rightarrow \frac{E}{R}\left(\frac{1}{T_2} - \frac{1}{T_1}\right) \\ &= \ell nt_2 - \ell nt_1 \end{aligned} \tag{12}$$

This result implies that the cure times to reach a specific T_g during the cure at two different temperatures differ by a constant amount, $S(T)$, on a logarithmic scale, which is equal to:

$$S(T) = \frac{E}{R}\left(\frac{1}{T_2} - \frac{1}{T_1}\right) \tag{13}$$

Table I Results from the Application of Eq. (7) to Model the T_g-Conversion Relationship for All Resin Systems

Resin	T_{g0} (°C)	$T_{g\infty}$ (°C)	λ
RTM6	−11	206	0.435
RMO	−11	208	0.677
RMO2	−21	193	0.847
F934	7	208	1.000

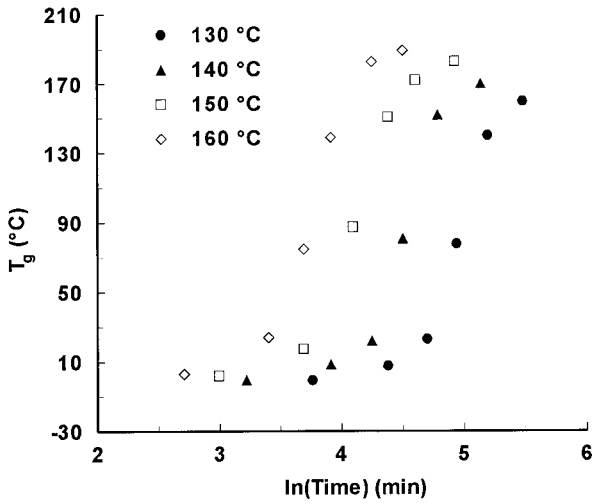

Figure 4 Plots of T_g against the natural logarithm of cure time for the isothermal cure of RMO2 resin at different cure temperatures.

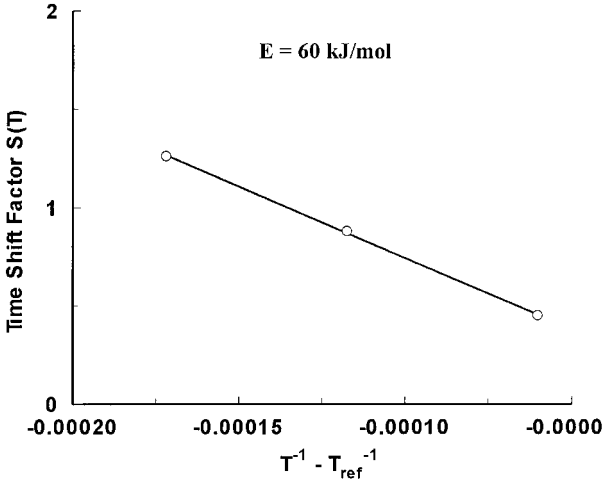

Figure 6 Arrhenius plot of the shift factors, $S(T)$, used to construct the master curve in Figure 5. The reference temperature was 130°C.

To explore this idea, the experimental T_g values of the RMO2 resin have been plotted in Figure 4 as functions of cure time, on a logarithmic scale. These plots indicate that a horizontal shift of the curves relative to a reference cure temperature (e.g., 130°C) will make them superimpose to a master curve. The master curve produced by the horizontal shift of the curves relative to the 130°C data is shown in Figure 5. The coincidence is good up to the vitrification point, because above that point the cure is not chemically controlled. The shift factors used have been plotted in Figure 6 as a function of the differences between the inverse of the cure temperature and the inverse of the reference temperature. According to eq. (13), this plot should give a straight line with a slope equal to E/R.

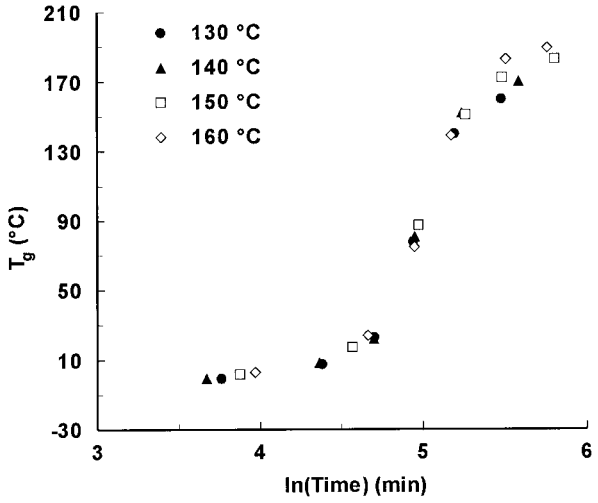

Figure 5 Superposition of the T_g vs. ℓn(time) RMO2 resin data by horizontal shifting of the original curves to form a master curve.

The activation energy for the curing reaction, as calculated from the slope of the Arrhenius plot in Figure 6, is 60 kJ/mol. The existence of a master curve for the T_g development and the Arrhenius dependence of the shift factors on temperature suggest that this resin system follows one overall reaction mechanism with a single apparent activation energy. This contradicts the results obtained from the reaction kinetics (see ref. 15), where two activated reaction mechanisms were obtained. The explanation for this discrepancy lies in the form of the expression used to describe the correlation between T_g and conversion [see eq. (7)]. Although there exists a one-to-one relationship between these two properties, that does not mean that this relationship is linear. These two properties are related by a proportionality function only, and only when the parameter λ in eq. (7) is equal to 1. Then, this expression can be written as:

$$T_g = T_{g0} + (T_{g\infty} - T_{g0})\alpha \qquad (14)$$

which expresses a linear dependence of T_g on conversion. Thus, any change in conversion has a similar effect on T_g. For the RMO2 resin, this is not the case. The parameter λ is equal to 0.847 (see Table I); thus, the proportionality law does

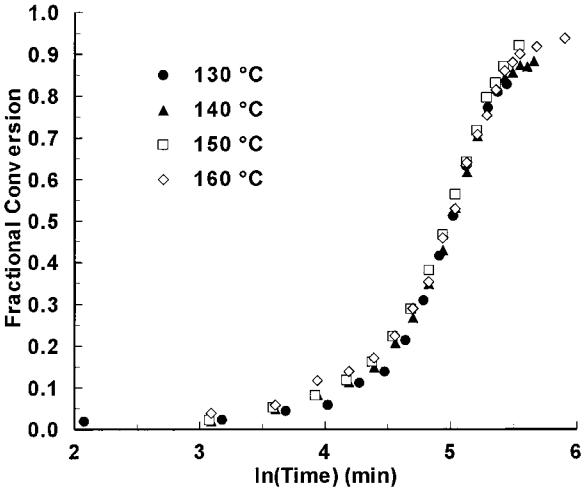

Figure 7 Superposition of the conversion vs. ℓn(time) data for the isothermal cure of RMO2 resin.

not hold. The above can be demonstrated easily by plotting conversion as a function of the natural logarithm of cure time. These plots are shown in Figure 7 for the isothermal cure of the RMO2 resin at different cure temperatures, horizontally shifted to produce a master curve. It is evident that these curves cannot be superimposed accurately at low conversions. At these conversions, the autocatalytic reaction mechanism is in control. If the curves were shifted to superimpose at these low conversions, then the high conversion data would have deviated from the master curve. At these high conversions, the noncatalytic reaction mechanism is in control.

The situation is different in the case of the F934 resin. As demonstrated in a previous publication (see ref. 15), this resin follows a single activated reaction mechanism (nth order kinetics) under isothermal conditions. This means that there should be a proportionality law describing the relation between T_g and conversion α for this resin.

Indeed, the results of the fit of eq. (7) to the experimental T_g data support this suggestion. The parameter λ was calculated to be equal to 1 (see Table I); thus, plotting conversion against the natural logarithm of cure time should produce a master curve. As shown in Figure 8, a master curve is followed for all cure temperatures. Deviations start to appear above the vitrification point, where the reaction is not chemically controlled but diffusion controlled.

From the above discussion it follows that eq. (9) does not always hold. What does hold, however, is that:

$$\frac{dT_g}{dt} = k(T)f(T_g) \tag{15}$$

because the T_g advancement follows a single activated mechanism for all the resin systems investigated. The above expression suggests that the T_g development should be treated in a completely different way than the reaction kinetics. The reaction kinetics are influenced by the chemical constituents of the reactive system, the possible interactions that can be established between them and the relative distances between the various reactive species as these are determined by the positions that they hold in space during the development of the three dimensional network. On the other hand, T_g seems to be influenced only by the structural configuration of the forming network itself and not by the possible reactions that can lead to this network.

Chemoviscosity Modeling

During an isothermal cure, the viscosity of a thermoset will increase continuously as a result of the extension of the molecular chains and the crosslinks that develop between them. As the gelation region is reached, the increase in viscosity becomes very high because of the formation of joint macromolecules extending throughout the resin mass. Thus, in a viscosity vs. cure time plot, the sudden increase in viscosity will mark the onset of gelation with the actual gelation usually occurring a few minutes after the onset has been reached. The characteristic viscosity profile given

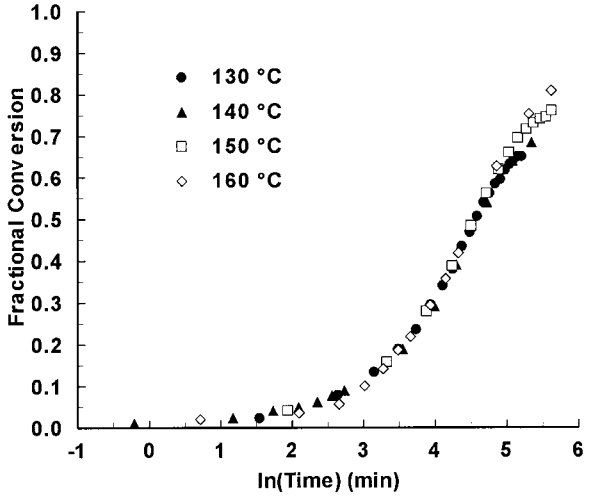

Figure 8 Superposition of the conversion vs. ℓn(time) data for the isothermal cure of F934 resin.

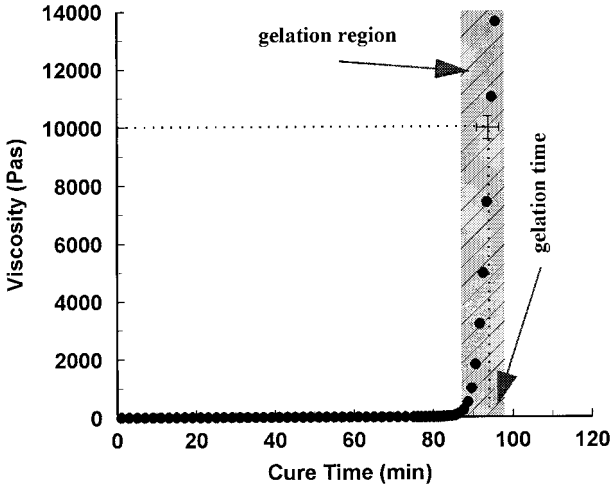

Figure 9 Viscosity profile of RTM6 resin cured isothermally at 140°C.

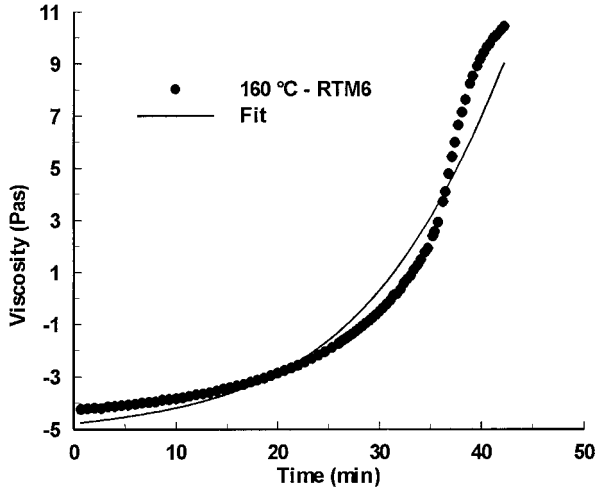

Figure 10 Application of eq. (17) and eq. (18) to model the experimental viscosity data of the isothermal cure of RTM6 resin at 160°C.

in Figure 9 is obtained from an isothermal cure of RTM6 resin at 140°C. As seen in this figure, the actual gelation region represents only a very small time period in the overall curing procedure. Thus, any time in this region will represent the actual gelation time to a satisfactory degree of accuracy. For reasons of reproducibility of gelation time values and for comparison between different cure temperatures and resin systems, the time needed to reach a viscosity value of 10 kPas will be taken here as the "operational" definition of gelation time.

The most commonly used mathematical expression to model viscosity data is the Williams-Landel-Ferry (WLF) equation and, especially for thermoset cure, a modified WLF equation,[13] given by eq. (6). The parameters that have to be evaluated are the constants C_1 and C_2. For the evaluation procedure to be more effective, the expression given by eq. (6) is transformed to the form:

$$1 = -C_1 \frac{1}{\ell n \eta - \ell n \eta_g} - C_2 \frac{1}{T_{\text{cure}} - T_g} \quad (16)$$

or, by substituting:

$$X_1 = -\frac{1}{\ell n \eta - \ell n \eta_g} \quad \text{and} \quad X_2 = -\frac{1}{T_{\text{cure}} - T_g} \quad (17)$$

to the form:

$$1 = C_1 X_1 + C_2 X_2 \quad (18)$$

The expression given by eq. (18) makes possible the use of multiple linear regression analysis to obtain the parameters C_1 and C_2 by treating the variables X_1 and X_2 as the independent variables.

The values of the independent variables X_1 and X_2 can be obtained easily from eq. (17), because all the variables involved are known; η is the experimentally obtained viscosity, T_{cure} is the temperature of the experiment, and T_g is the glass transition temperature, which can be obtained using the models developed in the previous section [see eq. (7)]. The value of η_g, (viscosity at

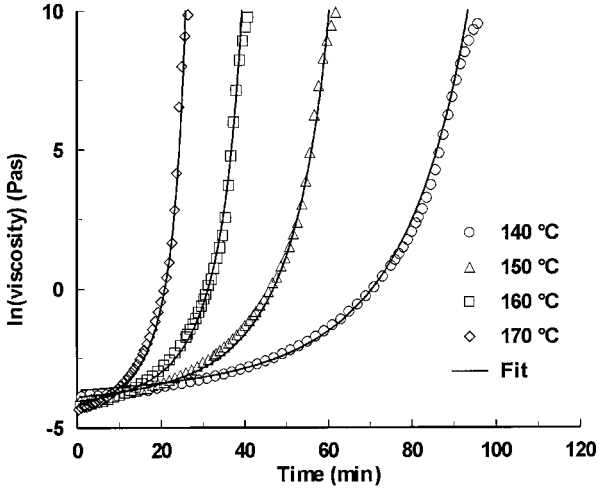

Figure 11 Application of eq. (18) and eq. (20) to model the experimental viscosity data of the isothermal cure of RTM6 resin at various cure temperatures.

Table II Best Fit Values of Parameters T_r, C_1, and C_2 of eq. (18) and eq. (20)

	Best Fit Lines		
Resin	T_r (°C)	ℓnC_1	ℓnC_2
RTM6	$-145 + 1.239 \cdot T_{\text{cure}}$	$2.908 + 291.8 \cdot T^{-1}$	$-5.485 + 3562 \cdot T^{-1}$
RMO	$-162 + 1.289 \cdot T_{\text{cure}}$	$3.120 + 185.0 \cdot T^{-1}$	$-5.964 + 3617 \cdot T^{-1}$
RMO2	$-196 + 1.243 \cdot T_{\text{cure}}$	$3.502 + 9.644 \cdot T^{-1}$	$-1.120 + 1602 \cdot T^{-1}$
F934	$-137 + 1.096 \cdot T_{\text{cure}}$	$3.240 + 251.5 \cdot T^{-1}$	$2.785 + 724 \cdot T^{-1}$

T_g) was taken from values obtained from the literature as 10^{12} Pas.[13]

The application of eq. (17) and eq. (18) to model the experimental data of the isothermal cure of RTM6 resin at 160°C produced the fit shown in Figure 10. The calculated parameters C_1 and C_2 had the values 45.46 and 68.72, respectively. The observed deviation of the fitting from the experimental data suggests that some modifications need to be made to the model. The modified model that was used has the form:

$$\ell n \frac{\eta}{\eta_g} = -\frac{C_1(T_{\text{cure}} - T_r - T_g)}{C_2 + T_{\text{cure}} - T_r - T_g} \qquad (19)$$

where T_r is a reference temperature, which can be treated as an adjustable parameter.

This form of viscosity model has been used successfully by Gillham and coworkers.[16] Transformation of this model will give the same general expression as that given by eq. (18), but with the new variables X_1' and X_2' given by:

$$X_1' = -\frac{1}{\ell n \eta - \ell n \eta_g}$$

$$\text{and} \qquad X_2' = -\frac{1}{T_{\text{cure}} - T_r - T_g} \qquad (20)$$

The application of eq. (18) and eq. (20) to the experimental data of RTM6 resin resulted in the fittings shown in Figure 11. The improvement of the fitting is evident. The simulation of the viscosity advancement is very successful up to gelation.

The calculated values of the parameters C_1, C_2, and T_r were found to depend on the cure temperature. The best fitted lines for all the parameters and for all our resin systems are given in Table II.

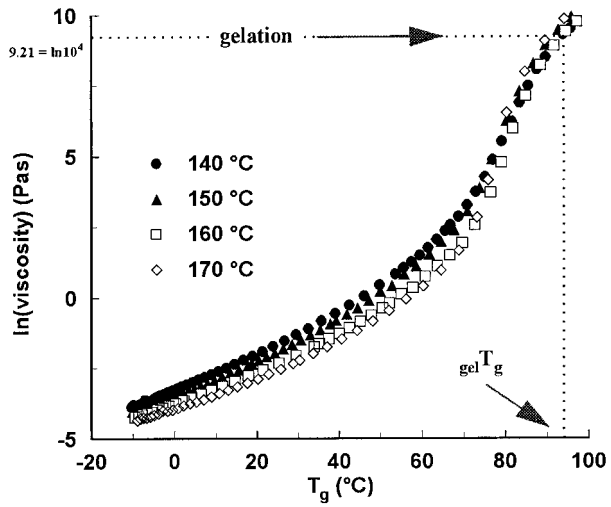

Figure 12 Viscosity vs. T_g for the isothermal cure of RTM6 resin at various cure temperatures. Gelation point is indicated.

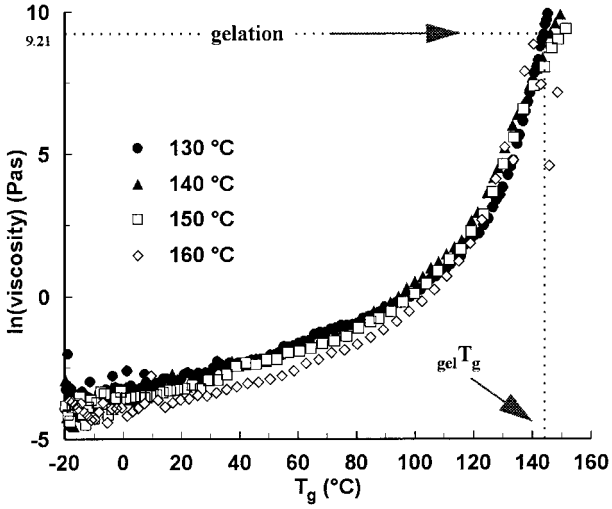

Figure 13 Viscosity vs. T_g for the isothermal cure of RMO2 resin at various cure temperatures. Gelation time is also indicated.

Table III Characteristic Points at Gelation for Different Isothermal Cures

	Gelation Time (t_{gel}/min)						
Resin	130°C	140°C	150°C	160°C	170°C	$_{gel}T_g$ (°C)	α_{gel}
RTM6	—	95	61	40	26	94	0.59
RMO	—	117	72	48	32	105	0.62
RMO2	215	132	87	56	—	144	0.80
F934	87	51	30	18	—	100	0.47

Some deviation from linearity is observed in the case of the RMO2 resin. To have a better insight into the way the evaluated parameters reflect the differences in structure between the different resin systems, viscosity was plotted against T_g advancement for all resins. These plots are shown in Figures 12 and 13 for the RTM6 and RMO2 resin systems, respectively.

It is evident from the plots that the viscosity profiles converge at a specific point and then diverge again. The point of coincidence is very close to gelation (as defined by the attainment of 10^4 Pas). At a specific T_g, the viscosity is higher at lower cure temperatures. As the cure progresses, the differences in viscosity between different cure temperatures at specific T_g values become smaller, and the curves slowly converge to a specific point at gelation. The approximate T_g values at gelation and the corresponding conversions for all resins are given in Table III together with the cure times required to reach gelation at each cure temperature.

A close inspection of these values reveals that for the RMO2 resin system gelation occurs at a conversion level of about 80%, which corresponds to a T_g of about 144°C. This means that the cure had already reached the vitrification point for the two low cure temperatures (130 and 140°C). Thus, the cure has become diffusion controlled prior to gelation. This could explain the deviation from linearity observed for the estimated parameters of the viscosity model for that particular resin system.

CONCLUSIONS

The analysis of T_g profiles revealed that a single activation mechanism is followed during the build-up of the three-dimensional network, in contrast to the reaction kinetics, which follow several activation mechanisms depending on the nature of the individual cure reaction. The results concerning T_g advancement can be summarized as follows: (i) the glass transition temperature advancement during the cure follows the same trend as the reaction advancement; (ii) a one-to-one relationship exists between T_g and conversion, suggesting that the formed network is independent of the conditions under which the cure reactions occur; and (iii) all the resin systems vitrify under isothermal conditions without reaching 100% conversion.

Viscosity changes were also monitored during the cure of each resin system. Application of a modified version of the WLF equation was very successful in the modeling of the viscosity data. All the parameters of the equation were found to depend on the cure temperature in a systematic manner. The physical transformation from the liquid to the rubbery state (gelation) was detected from the viscosity profiles. Further combination of the viscosity results with the cure kinetics results and the T_g results suggests that gelation occurs at a specific T_g, which is unique for each resin system.

The authors acknowledge financial support for P.I.K. from the industrial partners in DTI/EPSRC LINK Structural Composites project "PORPPC" (GR/J96222). Gifts of materials from Hexcel Composites (UK) and ICI Fiberite (Europe) as well as numerous discussions with Professor (Emeritus) H. Block and Dr. G. M. Maistros are also gratefully ackowledged.

REFERENCES

1. Ferry, J. D. Viscoelastic Properties of Polymers; J. Wiley and Sons: New York, 1980, 3rd ed.
2. Simon, S. L.; Gillham, J. K. J Appl Polym Sci 1994, 53, 709.
3. Adabbo, E.; Williams, R. J. J. J Appl Polym Sci 1982, 27, 1327.
4. Nielsen, L. E. J Macromol Sci Rev Macromol Chem 1969, C3, 69.

5. Roller, M. B. Polym Eng Sci 1986, 26, 432.
6. Cheng, K. C.; Chiu, W. Y.; Hsieh, K. H.; Ma, C. C. M. J Mater Sci 1994, 29, 721.
7. Mijovic, J.; Hung Lee, C. J Appl Polym Sci 1989, 38, 2155.
8. Lipshitz, S. D.; Macosko, C. W. Polym Eng Sci 1976, 16, 803.
9. Castro, J. M.; Macosko, C. W. Soc Plast Eng Tech Papers 1980, 26, 434.
10. Perry, M. J.; James Wang, T.; Ma, Y.; James Lee, L. 24th Int SAMPE Tech Conf 1992, 24, 421.
11. Bidstrup, S. A.; Macosko, C. W. J Polym Sci Part B Polym Phys 1990, 28, 691.
12. Williams, M. L.; Landel, R. F.; Ferry, J. D. J Am Chem Soc 1955, 77, 3701.
13. Mijovic, J.; Hung Lee, C. J Appl Polym Sci 1989, 37, 889.
14. Halley, P. J.; Mackay, M. E. Polym Eng Sci 1996, 36, 593.
15. Karkanas, P. I.; Partridge, I. K. J Appl Polym Sci 2000, 77, 1419.
16. Enns, J. B.; Gillham, J. K. J Appl Polym Sci 1983, 28, 2567.